Journal of Organometallic Chemistry, 363 (1989) 181–188
Elsevier Sequoia S.A., Lausanne – Printed in The Netherlands
JOM 09454

High nuclearity carbonyl clusters of rhodium. Synthesis and crystal structure of $(NMe_4)_3[Rh_{14}H(CO)_{25}] \cdot Me_2CO$

Gianfranco Ciani*, Massimo Moret, and Angelo Sironi

Istituto di Chimica Strutturistica Inorganica and Centro C.N.R., Via G. Venezian 21, 20133 Milano (Italy)

and Secondo Martinengo*

Centro del C.N.R. di Studio della Sintesi e Struttura dei Composti dei Metalli di Transizione nei Bassi Stati di Ossidazione, Via G. Venezian 21, 20133 Milano (Italy)

(Received July 27th, 1988)

Abstract

The compound $(NMe_4)_3[Rh_{14}H(CO)_{25}] \cdot Me_2CO$ has been obtained by treatment of $(NMe_4)_4[Rh_{14}(CO)_{25}]$ with acids. The $(NMe_4)^+$ salt of the trianion, containing solvated acetone molecules, crystallizes in the orthorhombic *Pmcn* space group (non-standard setting of *Pnma*, No. 62), with *a* 16.436(2), *b* 17.655(4), *c* 21.490(4) Å and $Z = 4$. The structure was refined by full-matrix least-squares, on the basis of 3472 significant unique reflections, to a final *R* value of 0.056. The anion shows a structure related to that of the parent $[Rh_{14}(CO)_{25}]^{4-}$, which is a distorted fragment of body-centered cubic packing with C_{4v} symmetry. However, the insertion of the hydride ligand in an interstitial position, confirmed also by NMR studies, causes significant changes both in the metallic skeleton and in the CO stereochemistry, reducing the overall symmetry to C_s. The Rh–Rh distances are scattered. The central metal exhibits 8 short (mean 2.657 Å), two normal (2.878(1) Å) and three very long (mean 3.258 Å) contacts with the surface metals. The Rh–Rh surface interactions range from 2.692(1) to 3.356(2) Å. The metal atom polyhedron can be described as intermediate between a body-centered cubic and a closest-packed entity. The carbonyl ligands are bound 10 terminally (mean Rh–C and C–O 1.86 and 1.15 Å), 13 almost symmetric double-bridging (mean Rh–C and C–O 2.01 and 1.17 Å), and two markedly asymmetric double-bridging (short Rh–C 1.89(2), long Rh–C 2.41(2) and C–O 1.16(2) Å). The structure is compared with those of related high-nuclearity rhodium clusters.

Introduction

One of the aims of our studies on high nuclearity carbonyl clusters of rhodium has been to ascertain that these species contain metal arrangements which are

0022-328X/89/$03.50

fragments of metallic lattices and, therefore could serve as models for small metallic crystallites (covered by ligands) in elucidation of the understanding of the mechanisms of metal atoms aggregation and of the interactions of metal surfaces with small molecules. All these features may be of relevance from a catalytic point of view.

With the exception of cluster species containing main group interstitial elements, which can assume less compact metallic arrays, compact closest-packed geometries are usually observed. This is the case for the hexagonal closest-packed $[Rh_9(CO)_{19}]^{3-}$ [1], $[Rh_{10}(CO)_{21}]^{2-}$ [2], $[Rh_{12}H_2(CO)_{25}]$ [3], the family $[Rh_{13}H_{5-n}(CO)_{24}]^{n-}$ ($n = 2$ [4], 3 [5], 4 [6]), and $[Rh_{17}(CO)_{30}]^{3-}$ [7]. A mixed hexagonal/cubic closest-packing was observed in the large $[Rh_{22}(CO)_{37}]^{4-}$ anion [8]. A metallic lattice less compact for closest-packing is the body-centered cubic, observed, with some distortions, in $[Rh_{14}(CO)_{25}]^{4-}$ [9,10], in $[Rh_{22}H_x(CO)_{35}]^{n-}$ ($n = 4$, 5 [11]) and, almost regular, in $[Rh_{15}(CO)_{30}]^{3-}$ [12]. Intermediate situations representing body-centered/closest-packed rearrangements have been found in $[Rh_{14}(CO)_{26}]^{2-}$ [13], in $[Rh_{15}(CO)_{27}]^{3-}$ [9] and in the hydride $[Rh_{14}H(CO)_{25}]^{3-}$ [14].

The latter anion has now been reinvestigated. A preliminary account of its preparation, reactivity, and structural characterization as $(NEt_4)^+$ salt has appeared [14]. However, since that structure was of rather poor quality we have now undertaken a new X-ray study with a different cation in order to get better structural parameters. We describe here the result of a single crystal investigation on its tetramethylammonium salt. The structural parameters are compared with those of the related rhodium cluster compounds, and the indirect location of the hydride ligand is discussed in connection with the data from variable temperature NMR studies [15a,b].

Results and discussion

We have previously reported that the $[Rh_{14}H(CO)_{25}]^{3-}$ anion can be obtained in different reactions, namely the protonation of the corresponding tetraanion [14], the condensation of the cation $[Rh(CO)_2(MeCN)_2]^+$ with the $[Rh_{13}H(CO)_{24}]^{4-}$ tetraanion [14] or the nucleophilic attack of OH^- ions on the $[Rh_{14}(CO)_{26}]^{2-}$ anion [13]. We can now add that the $[Rh_{14}H(CO)_{25}]^{3-}$ anion is also partially formed on simple hydrolysis of $[Rh_{14}(CO)_{25}]^{4-}$; thus on dissolution of the tetraanion in MeCN containing 2% of water, an equilibrium mixture of $[Rh_{14}H(CO)_{25}]^{3-}$ and $[Rh_{14}(CO)_{25}]^{4-}$, in about the 1/1 ratio, is slowly formed according to eq. 1.

$$[Rh_{14}(CO)_{25}]^{4-} + H_2O \leftrightarrows [Rh_{14}H(CO)_{25}]^{3-} + OH^- \quad (1)$$

Use of larger amounts of water increases the amount of the hydridic species. Equilibria such as in eq. 1 are relevant in certain catalytic reactions, and the $[Rh_{14}(CO)_{25}]^{4-}$ anion has been found in catalytic systems based on aminated polystyrene-bound Rh clusters active in the water gas shift reaction [16].

The $(NMe_4)_3[Rh_{14}H(CO)_{25}]$ salt we used in this work was prepared as previously described [15b] by protonation of $[NMe_4]_4[Rh_{14}(CO)_{25}]$ with phosphoric acid in MeCN solution. The IR spectrum of the pure product in MeCN shows bands at 1992vs and 1835m cm^{-1}. Although solutions of the product are readily oxidized in air, the crystals were sufficiently stable to allow X-ray data collection without protection.

Description of the structure

The crystal structure involves packing of discrete $[Rh_{14}H(CO)_{25}]^{3-}$ anions, tetramethylammonium cations and solvated acetone molecules in the ratio 1/3/1. The anion lies on a crystallographic mirror plane and exhibits an overall C_s symmetry. The cluster of bare metal atoms and the anion are illustrated in Fig. 1 and 2, respectively. Interatomic distances and angles are given in Table 1. The Rh_{14} polyhedron (Fig. 1) is related to that of the parent $[Rh_{14}(CO)_{25}]^{4-}$ anion (**1**), which can be described as a somewhat distorted body-centered cubic fragment, of C_{4v} symmetry [10]. The presence of a hydride ligand reduces the symmetry, so that only one of the original mirror planes is retained. The principal distortions in the metal array are shown in Table 2. In both cases the central metal is surrounded by 8 nearest neighbours, which define in **1** a distorted tetragonal metallic prism (mean Rh–Rh in the basal uncapped square and in the capped square of 2.793 and 2.992 Å, respectively) markedly elongated in the direction of the four-fold axis (mean Rh–Rh 3.325 Å). The cluster geometry is more regular in the anion $[Rh_{15}(CO)_{30}]^{3-}$ [12], of idealized O_h symmetry, which represents a rhombic dodecahedron, i.e. an almost undistorted fragment of body-centered cubic lattice, with the central metal showing 8 short bonds (mean 2.604 Å) and 6 long contacts (mean 3.250 Å).

The metal atom polyhedron in $[Rh_{14}H(CO)_{25}]^{3-}$, with 10 definitely bonding Rh–Rh contacts between the central and the surface metals, can be described as intermediate between a body-centered cubic (bcc) and a closest-packed (cp) fragment. The bcc moiety involves atoms Rh(0), Rh(1), Rh(2), Rh(7), Rh(7′), Rh(5), Rh(5′), Rh(6), Rh(6′), and Rh(9), while the cp fragment is represented by two layers (Rh(0), Rh(5), Rh(5′), Rh(6), Rh(6′), Rh(9) and Rh(3), Rh(4), Rh(8), and Rh(8′)). Similar intermediate bcc/cp metal arrangements were also observed in species like $[Rh_{14}(CO)_{26}]^{2-}$ [13] and $[Rh_{15}(CO)_{27}]^{3-}$ [9].

The comparison of the metal cluster geometries in **1** and in $[Rh_{14}H(CO)_{25}]^{3-}$ clearly shows that the insertion of the hydride ligand occurs on the almost square face Rh(3,4,8,8′) (mean acute and obtuse Rh–Rh–Rh angles of 83.9 and 95.9°), i.e. in a slightly distorted [100] surface hole of the cp moiety, as can be inferred from the marked lengthening of the Rh(3)–Rh(4) distance compared with that in the parent

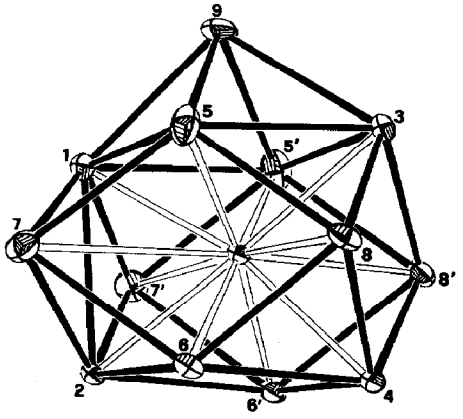

Fig. 1. A view of the bare Rh_{14} metal atom cluster (the central metal atom is named Rh(0)). A crystallographic mirror plane passes through atoms Rh(0), Rh(1), Rh(2), Rh(3), Rh(4) and Rh(9).

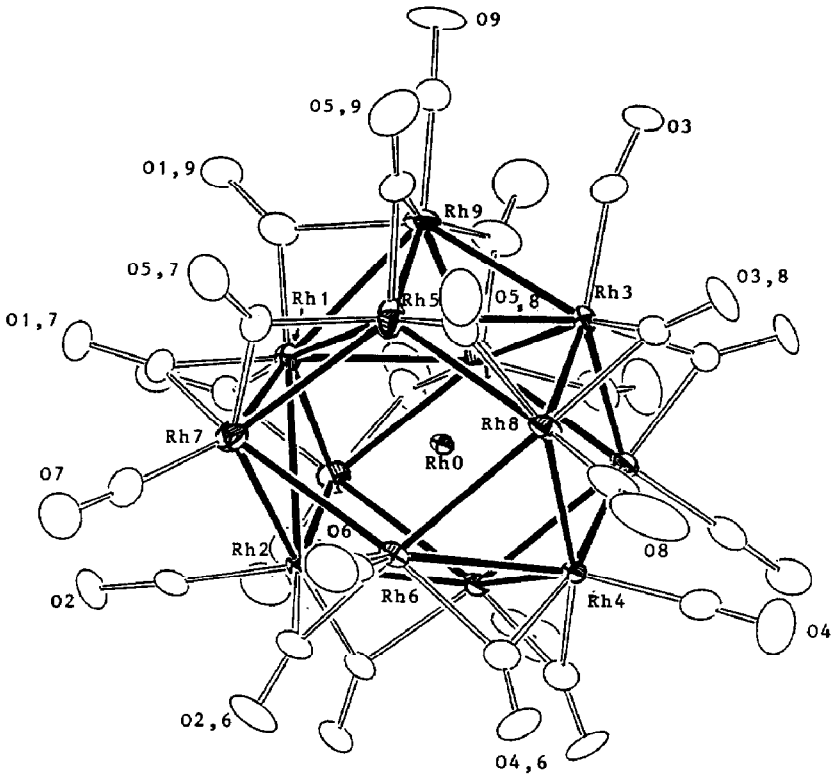

Fig. 2. A view of the anion $[Rh_{14}H(CO)_{25}]^{3-}$. The carbonyl ligands are indicated by the numbers of their oxygen atoms.

anion. This semi-interstitial location is reminiscent of those suggested for the hydrides of the family $[Rh_{13}H_{5-n}(CO)_{24}]^{n-}$. These lateral faces of **1**, relatively less crowded than the others, are the preferred sites of attack by electrophilic reagents since the cation $[Rh(CO)_2(NCMe)_2]^+$ also bonds to one of them to give $[Rh_{15}(CO)_{27}]^{3-}$. The bcc → cp cluster interconversion of $[Rh_{14}H(CO)_{25}]^{3-}$ due to insertion of the hydride ligand is a feature also observed in binary hydrides of transition metals [17].

The ^1H-{^{103}Rh} INDOR NMR spectra at −80 °C are consistent with our suggested position of the hydride ligand; at this temperature, an interstitial H migration occurs within the four lateral distorted semi-octahedral cavities [15a,b].

The carbonyl stereochemistry differs from that of the parent anion **1**. The CO ligands are bound 10 terminally (mean Rh–C and C–O 1.86 and 1.15 Å), 13 almost symmetric double-bridging (mean Rh–C and C–O 2.01 and 1.17 Å), and two markedly asymmetric double-bridging, on edges Rh(5)–Rh(9) and Rh(5′)–Rh(9), (short Rh–C 1.89(2), long Rh–C 2.41(2) and C–O 1.16(2) Å).

The $[Rh_{14}H(CO)_{25}]^{3-}$ anion possesses 180 valence electrons, corresponding to 90 cluster valence molecular orbitals (cvmos). We have previously suggested [18] that the number of cvmos for a carbonyl cluster could be estimated using the equation $6N + X$, with N = number of metals and X = a number depending on the compactness of the metallic array. For compact closest-packed clusters X usually has a value of $7(\pm 1)$, whatever the number of metals. In the three Rh_{14} anions and in

Table 1

Bond distances (Å) and angles (deg.) in $[Rh_{14}H(CO)_{25}]^{3-}$

Bond distances			
Rh(0)–Rh(1)	2.617(2)	Rh(8)–C(8)	1.82(2)
Rh(0)–Rh(2)	2.672(1)	Rh(9)–C(9)	1.86(2)
Rh(0)–Rh(3)	2.680(1)	Rh(1)–C(1,7)	2.02(1)
Rh(0)–Rh(4)	2.670(1)	Rh(7)–C(1,7)	1.95(1)
Rh(0)–Rh(5)	2.637(1)	Rh(1)–C(1,9)	1.92(2)
Rh(0)–Rh(6)	2.672(1)	Rh(9)–C(1,9)	2.09(2)
Rh(0)...Rh(7)	3.233(1)	Rh(2)–C(2,6)	2.04(1)
Rh(0)–Rh(8)	2.878(1)	Rh(6)–C(2,6)	2.01(1)
Rh(0)...Rh(9)	3.308(2)	Rh(3)–C(3,8)	1.96(1)
Rh(1)–Rh(2)	3.047(2)	Rh(8)–C(3,8)	2.07(1)
Rh(1)–Rh(5)	3.029(1)	Rh(4)–C(4,6)	2.06(1)
Rh(1)–Rh(7)	2.708(1)	Rh(6)–C(4,6)	2.03(1)
Rh(1)–Rh(9)	2.744(2)	Rh(5)–C(5,7)	2.00(1)
Rh(2)–Rh(6)	2.796(1)	Rh(7)–C(5,7)	2.01(1)
Rh(2)–Rh(7)	2.788(1)	Rh(5)–C(5,8)	1.92(2)
Rh(3)...Rh(4)	3.649(2)	Rh(8)–C(5,8)	2.06(2)
Rh(3)–Rh(5)	3.023(1)	Rh(5)–C(5,9)	1.89(2)
Rh(3)–Rh(8)	2.736(1)	Rh(9)–C(5,9)	2.41(2)
Rh(3)–Rh(9)	2.787(2)	C(2)–O(2)	1.17(2)
Rh(4)–Rh(6)	2.781(1)	C(3)–O(3)	1.12(2)
Rh(4)–Rh(8)	2.720(1)	C(4)–O(4)	1.11(3)
Rh(5)...Rh(6)	3.356(2)	C(6)–O(6)	1.17(2)
Rh(5)–Rh(7)	2.738(2)	C(7)–O(7)	1.14(2)
Rh(5)–Rh(8)	2.692(1)	C(8)–O(8)	1.19(2)
Rh(5)–Rh(9)	2.773(2)	C(9)–O(9)	1.14(3)
Rh(6)–Rh(7)	2.807(1)	C(1,7)–O(1,7)	1.20(1)
Rh(6)–Rh(8)	2.740(1)	C(1,9)–O(1,9)	1.21(3)
Rh(2)–C(2)	1.84(2)	C(2,6)–O(2,6)	1.15(1)
Rh(3)–C(3)	1.94(2)	C(3,8)–O(3,8)	1.19(1)
Rh(9)...C(3)	2.70(2)	C(4,6)–O(4,6)	1.08(1)
Rh(4)–C(4)	1.85(2)	C(5,7)–O(5,7)	1.18(1)
Rh(6)–C(6)	1.85(2)	C(5,8)–O(5,8)	1.19(2)
Rh(7)–C(7)	1.87(2)	C(5,9)–O(5,9)	1.16(2)
Bond angles			
Rh(2)–C(2)–O(2)	177 (2)	Rh(2)–C(2,6)–Rh(6)	87.3(5)
Rh(3)–C(3)–O(3)	165 (2)	Rh(3)–C(3,8)–O(3,8)	142 (1)
Rh(9)–C(3)–O(3)	123 (1)	Rh(8)–C(3,8)–O(3,8)	132 (1)
Rh(4)–C(4)–O(4)	178 (2)	Rh(3)–C(3,8)–Rh(8)	85.6(4)
Rh(6)–C(6)–O(6)	174 (1)	Rh(4)–C(4,6)–O(4,6)	133 (1)
Rh(7)–C(7)–O(7)	176 (2)	Rh(6)–C(4,6)–O(4,6)	141 (1)
Rh(8)–C(8)–O(8)	172 (2)	Rh(4)–C(4,6)–Rh(6)	85.7(5)
Rh(9)–C(9)–O(9)	178 (2)	Rh(5)–C(5,7)–O(5,7)	137 (1)
Rh(1)–C(1,7)–O(1,7)	136 (1)	Rh(7)–C(5,7)–O(5,7)	136 (1)
Rh(7)–C(1,7)–O(1,7)	138 (1)	Rh(5)–C(5,7)–Rh(7)	86.3(5)
Rh(1)–C(1,7)–Rh(7)	86.1(4)	Rh(5)–C(5,8)–O(5,8)	144 (1)
Rh(1)–C(1,9)–O(1,9)	142 (2)	Rh(8)–C(5,8)–O(5,8)	130 (1)
Rh(9)–C(1,9)–O(1,9)	132(2)	Rh(5)–C(5,8)–Rh(8)	85.0(6)
Rh(1)–C(1,9)–Rh(9)	86.4(9)	Rh(5)–C(5,9)–O(5,9)	152 (2)
Rh(2)–C(2,6)–O(2,6)	134 (1)	Rh(9)–C(5,9)–O(5,9)	129 (2)
Rh(6)–C(2,6)–O(2,6)	138 (1)	Rh(5)–C(5,9)–Rh(9)	79.3(7)

Table 2

A comparison of the Rh–Rh interactions (Å) between $[Rh_{14}(CO)_{25}]^{4-}$ (1) and $[Rh_{14}(CO)_{25}]^{3-}$ (2)

Anion	1	2
Central-to-surface	8 short bonds (2.638)	8 short bonds (2.657)
	4 long bonds with the lateral caps (3.076)	2 normal bonds with 2 lateral caps (2.878) 2 very long contacts with 2 lateral caps (3.233)
	1 very long contact with the apical cap (3.372)	1 very long contact with the apical cap (3.308)
Surface-to-surface	4 normal bonds in the basal uncapped square (2.793)	4 normal bonds in the basal uncapped square (2.789)
	4 long bonds in the opposite capped square (2.992)	4 long bonds in the opposite capped square (3.026)
	16 normal bonds involving the lateral caps (2.740)	16 normal bonds involving the lateral caps (2.741)
	4 normal bonds involving the apical cap (2.791)	4 normal bonds involving the apical cap (2.769)
	4 very long contacts between basal and opposite square (3.325)	1 long contact between basal and opposite square (3.047) 2 very long contacts between basal and opposite square (3.356) – the other distance between the two squares is definitely non bonding (3.649)

$[Rh_{15}(CO)_{27}]^{3-}$ X has a value of 6. Since these species show bcc packing, i.e. less compact than the closest-packing, a value of X higher than 7 would be expected. Such a higher value is found for the anion $[Rh_{15}(CO)_{30}]^{3-}$, which represents an almost undistorted fragment of body-centered cubic lattice, and has an X value of 9. The low X values for the other species are very probably due to their incomplete modelling of a bcc fragment, which leads to distortions that increase significantly the compactness of the metallic skeleton.

Experimental

Preparation of $[NMe_4]_3[Rh_{14}H(CO)_{25}]$

$[NMe_4]_3[Rh_{14}H(CO)_{25}]$ was prepared as described for the tetramethylammonium salt [15b] by using the corresponding tetramethylammonium parent compound, the only difference being that, owing to the higher solubility of the $[NMe_4]^+$ salt further concentration in vacuum was required to complete the precipitation of the product. Crystals suitable for the X-ray analysis were obtained in the following way: ca. 0.1 g of the crude product, was dissolved in acetone (0.6 ml); MeOH was cautiously

added dropwise to the stirred solution until a slight turbidity was produced (ca. 4 ml), then a layer of 2-propanol (16 ml) was placed over the solution, and the solvents left to diffuse. The mother liquor was removed by syringe, and the crystals were washed with 2-propanol and vacuum dried.

X-ray analysis

Crystal data. $C_{40}H_{43}N_3O_{26}Rh_{14}$, $M = 2422.5$, orthorhombic, space group *Pmcn* (non-standard setting of *Pnma*, No. 62), with a 16.436(2), b 17.655(4), c 21.490(4) Å, U 6235.9 Å^3, $F(000)$ 4568, D_c 2.580 g cm^{-3} for $Z = 4$; Mo-K_α radiation (λ 0.71073 Å), μ (Mo-K_α) 36.2 cm^{-1}.

Intensity measurements. A crystal of dimensions of 0.12 × 0.14 × 0.31 mm was mounted on a glass fibre in the air. The intensity data were collected on an Enraf–Nonius CAD4 automated diffractometer, using graphite monochromatized Mo-K_α radiation. The setting angles of 25 random intense reflections ($16 < 2\vartheta < 25°$) were used to determine accurate cell constants and orientation matrix by least-squares. The data collection was performed by the ω-scan method, within the limits $3 < \vartheta < 25°$. A variable scan-speed (from 2 to 20°/min) and a variable scan-range of $(1.2 + 0.35 \tan \vartheta)°$ were used, with a 25% extension at each end of the scan-range for background determination. The total number of collected reflections was 5698. Three standard intense reflections, measured at regular intervals,

Table 3

Final positional parameters for $(NMe_4)_3[Rh_{14}H(CO)_{25}]\cdot Me_2CO$

Atom	x	y	z	Atom	x	y	z
Rh(0)	0.250	−0.04127(7)	0.29685(5)	C(1,9)	0.250	−0.130(2)	0.123(1)
Rh(1)	0.250	−0.04185(9)	0.17509(7)	O(1,9)	0.250	−0.149(1)	0.0693(7)
Rh(2)	0.250	0.10109(7)	0.25458(6)	C(2,6)	0.1591(9)	0.1523(7)	0.3034(6)
Rh(3)	0.250	−0.18552(8)	0.33569(6)	O(2,6)	0.1373(6)	0.2140(5)	0.3089(5)
Rh(4)	0.250	−0.00432(8)	0.41732(6)	C(3,8)	0.1675(9)	−0.2050(8)	0.3994(6)
Rh(5)	0.11992(8)	−0.11315(8)	0.25596(5)	O(3,8)	0.1430(7)	−0.2528(5)	0.4334(5)
Rh(6)	0.13061(6)	0.04917(5)	0.33685(5)	C(4,6)	0.1611(9)	0.0774(8)	0.4254(7)
Rh(7)	0.11115(8)	0.03031(7)	0.20799(5)	O(4,6)	0.1462(7)	0.1170(7)	0.4617(4)
Rh(8)	0.12671(7)	−0.09668(6)	0.38037(5)	C(5,7)	0.038(1)	−0.0603(9)	0.2028(7)
Rh(9)	0.250	−0.1926(1)	0.20611(8)	O(5,7)	−0.0232(7)	−0.0755(7)	0.1772(6)
C(2)	0.250	0.164(1)	0.186(1)	C(5,8)	0.0409(9)	−0.137(1)	0.3188(8)
O(2)	0.250	0.2012(9)	0.1410(7)	O(5,8)	−0.0270(8)	−0.1569(9)	0.3276(6)
C(3)	0.250	−0.288(1)	0.3041(9)	C(5,9)	0.105(1)	−0.209(1)	0.2181(8)
O(3)	0.250	−0.3513(8)	0.2990(7)	O(5,9)	0.064(1)	−0.259(1)	0.2021(7)
C(4)	0.250	−0.031(1)	0.501(1)	N(1)	0.0486(7)	0.3083(7)	0.4801(5)
O(4)	0.250	−0.045(2)	0.5509(9)	CT11	0.065(1)	0.269(1)	0.5391(8)
C(6)	0.020(1)	0.0678(8)	0.3457(8)	CT12	0.006(1)	0.381(1)	0.4912(9)
O(6)	−0.0497(6)	0.0729(8)	0.3519(7)	CT13	0.126(1)	0.329(1)	0.4485(9)
C(7)	0.033(1)	0.103(1)	0.1860(7)	CT14	0.001(1)	0.256(1)	0.4413(8)
O(7)	−0.017(1)	0.1439(9)	0.1725(7)	N(2)	0.250	0.422(1)	0.2152(9)
C(8)	0.068(1)	−0.0863(8)	0.4519(9)	CT21	0.250	0.406(3)	0.150(2)
O(8)	0.021(1)	−0.0786(8)	0.4936(7)	CT22	0.250	0.357(2)	0.252(2)
C(9)	0.250	−0.287(2)	0.168(1)	CT23	0.184(2)	0.471(2)	0.229(1)
O(9)	0.250	−0.344(1)	0.142(1)	OS	0.250	0.449(1)	0.3904(8)
C(1,7)	0.161(1)	0.0117(9)	0.1274(6)	CS	0.250	0.515(1)	0.4138(9)
O(1,7)	0.147(1)	0.0257(8)	0.0737(5)	CS1	0.172(1)	0.553(1)	0.4270(9)

showed no significant decay during the collection. The intensities were corrected for Lorentz and polarization effects. An empirical absorption correction was applied to the data set, based on ψ-scans (ψ 0–360° every 10°) of suitable reflections with χ values close to 90°; the maximum, minimum and average relative transmission factors were 1.00, 0.67 and 0.78, respectively. A set of 3472 independent significant reflections, with $I > 3\sigma(I)$, was used in the structure solution and refinement.

Structure solution and refinement. All computations were performed on a PDP 11/34 computer by use of the Enraf–Nonius Structure Determination Package (SDP). The metal atoms were located by direct methods. Successive difference-Fourier maps revealed the positions of all the remaining non-hydrogen atoms. The anion, one of the $(NMe_4)^+$ cations, and the solvated acetone molecule lie in special position, on a crystallographic mirror plane. The refinements were carried out by full-matrix least-squares. Anisotropic thermal factors were assigned to all atoms of the anion, while the remaining atoms were treated isotropically. The hydrogen atoms were neglected. The final difference-Fourier map was rather flat, showing some residual peaks not exceeding ca. 1 e $Å^{-3}$.

Weights were assigned according to the formula $w = 4F_o^2/\sigma(F_o^2)^2$, where $\sigma(F_o^2) = [\sigma(I)^2 + (pI)]^{1/2}/L_p$ (I and L_p being the integrated intensity and the Lorentz-polarization correction, respectively); p was optimized to 0.07. The final values of the conventional agreement indices R and R_w were 0.056 and 0.073, respectively; the error in an observation of unit weight was 1.589.

The final positional parameters are given in Table 3. The final thermal parameters and the list of observed and calculated structure factors can be obtained from the authors.

References

1 S. Martinengo, A. Fumagalli, R. Bonfichi, G. Ciani and A. Sironi, J. Chem. Soc., Chem. Commun., (1982) 825.
2 S. Martinengo, G. Ciani and A. Sironi, J. Chem. Soc., Chem. Commun., (1986) 1282.
3 G. Ciani, A. Sironi and S. Martinengo, J. Chem. Soc., Chem. Commun., (1985) 1757.
4 V.G. Albano, A. Ceriotti, P. Chini, G. Ciani, S. Martinengo and W.M. Anker, J. Chem. Soc., Chem. Commun., (1975) 859.
5 V.G. Albano, G. Ciani, S. Martinengo and A. Sironi, J. Chem. Soc., Dalton Trans., (1979) 978.
6 G. Ciani, A. Sironi and S. Martinengo, J. Chem. Soc., Dalton Trans., (1981) 519.
7 G. Ciani, A. Magni, A. Sironi and S. Martinengo, J. Chem. Soc., Chem. Commun., (1981) 1280.
8 S. Martinengo, G. Ciani and A. Sironi, J. Am. Chem. Soc., 102 (1980) 7565.
9 S. Martinengo, G. Ciani, A. Sironi and P. Chini, J. Am. Chem. Soc., 100 (1978) 7096.
10 G. Ciani, A. Sironi and S. Martinengo, J. Chem. Soc., Dalton Trans., (1982) 1099.
11 J.L. Vidal, R.C. Schoening and J.M. Troup, Inorg. Chem., 20 (1981) 227.
12 J.L. Vidal, L.A. Kapicak and J.M. Troup, J. Organomet. Chem., 215 (1981) C11.
13 S. Martinengo, G. Ciani and A. Sironi, J. Chem. Soc., Chem. Commun., (1980) 1140.
14 G. Ciani, A. Sironi and S. Martinengo, J. Organomet. Chem., 192 (1980) C42.
15 (a) B.T. Heaton, C. Brown, D.O. Smith, L. Strona, R.J. Goodfellow, P. Chini and S. Martinengo, J. Am. Chem. Soc., 102 (1980) 6175; (b) C. Allevi, B.T. Heaton, C. Seregni, L. Strona, R.J. Goodfellow, P. Chini and S. Martinengo, J. Chem. Soc., Dalton Trans., (1986) 1375.
16 K. Kaneda, M. Kobayashi, T. Imanaka and S. Teranishi, Chem. Lett., (1984) 1483.
17 A.F. Wells, Structural Inorganic Chemistry IV, Clarendon Press, Oxford, 1975, p. 294.
18 G. Ciani and A. Sironi, J. Organomet. Chem., 197 (1980) 233.